Arch. Metall. Mater. **68** (2023), 3, 1103-1108

DOI: https://doi.org/10.24425/amm.2023.145480

J. DUTKIEWICZ[1*], Ł. ROGAL[1], M. WĘGLOWSKI[2], T. CZUJKO[3], T. DUREJKO[3], E. CESARI[4]

COMPARISON OF MICROSTRUCTURE, AGEING EFFECT AND SHAPE MEMORY PROPERTIES OF ADDITIVELY MANUFACTURED NiTi ALLOY USING LENS AND EBAM METHODS

Samples prepared using various additive manufacturing methods were compared in terms of structure, texture, transformation temperature and superelastic properties. Samples manufactured using laser engineered net shaping (LENS) method showed texture several degrees deviated from the <001> build direction, however with composition near to the initial powder composition, enabling superelastic effect. The electron beam additive manufacturing (EBAM) samples showed martensitic structure at room temperature due to a shift of transformation temperatures to the higher range. This shift occurs due to a lower Ni content resulting from different processing conditions. However, EBAM method produced sharper <001> texture in the build direction and made it possible to obtain a good superelastic effect above room temperature. Intermetallic particles of size 0.5-2 mm were identified as Ti_2Ni phase using EDS and electron diffraction analyses. This phase was often formed at the grain boundaries. Contrary to the LENS method, the EBAM prepared samples showed Ni-rich primary particles resulted from different processing conditions that reduce the Ni content in the solid solution thus increase the martensitic transformation temperature. Ageing at 500°C allowed for shifting the martensitic transformation temperatures to the higher range in both, LENS and EBAM, samples. It resulted from the formation of Ni rich coherent precipitates. In samples prepared by both methods and aged at 500°C, the presence of martensite B19' twins was observed mainly on {011} B19' planes.

Keywords: Additive Manufacturing; Shape Memory Alloys; NiTi; TEM studies

1. Introduction

Additive manufacturing (AM) is gaining more attention in the recent years due to the possibility of fabricating metallic parts of complex shapes, difficult to produce by conventional techniques, [1,2]. During the AM process, elements are manufactured using an additive material in the form of powder or wire which is melted using a highly focused laser or electron beam. Based on the type of the additive material, AM techniques can be divided into powder bed-like selective laser melting (SLM), powder-feed laser engineered net shaping (LENS) and wire-feed, in the case of electron beam additive manufacturing (EBAM) [2]. In the case of powder-based techniques, spherical, pre-alloyed powders are used [3], although the use of a mixture of elemental powders is also possible [4]. The alloys that are difficult to cast and plastically form are shape memory (SM) NiTi alloys. Therefore, several works were published recently concerning AM [3-17] of these alloys. Additive manufacturing enables tailoring the SM response by controlling the microstructure at resolutions difficult through conventional NiTi processing methods [6,7]. In ref. [7] in-situ X-ray diffraction was used to determine the local transformation temperature along the thermally affected regions in a laser processed NiTi thin sheet. The resulting transformation temperatures gradient, related to a local chemical compositional changes through Ni depletion, as well as residual stress, explain the changes in microstructure and mechanical properties in additive manufactured NiTi parts. It was shown that using different sets of process parameters, the phase transformation temperatures of SLM built NiTi entities can be directly tailored [9]. The reason behind it attributed to the Ni loss by evaporation, that increases with applied energy density. It has been concluded in Ref. [9-11] that aging is an effective method to tailor the shape memory properties and to obtain superelasticity of SLM fabricated Ni-rich NiTi alloys.

[1] INSTITUTE OF METALLURGY AND MATERIALS SCIENCE, PAS, 25, REYMONTA STR., 30-059 KRAKOW, POLAND
[2] ŁUKASIEWICZ – INSTITUTE OF WELDING, BŁOGOSŁAWIONEGO CZESŁAWA 16-18, 44-100 GLIWICE, POLAND
[3] MILITARY UNIVERSITY OF TECHNOLOGY, 2, INSTITUTE OF MATERIALS SCIENCE AND ENGINEERING, GEN. S. KALISKIEGO STR., 00-908, WARSAW, POLAND
[4] UNIVERSITY OF BALEARIC ISLANDS, DEPARTMENT OF PHYSICS, E07122, PALMA DE MALLORCA, SPAIN

* Corresponding author: j.dutkiewicz@imim.pl

In the case of NiTi/TiC composites [10] three different lenticular Ni_4Ti_3 variants were found depending on precipitate diameters, causing the formation of a higher interface lattice strain energy between the smaller Ni_4Ti_3 variant and the matrix. Furthermore, as reported in Ref. [11] the heat treatment decreased the forward and reverse transformation temperatures of NiTi alloy, presumably due to the annihilation of thermally induced defects. The samples annealed at 500°C showed a measurable increase of the shape memory recovery, as compared to the as-processed NiTi alloy. Additionally, the pseudoelastic recoverability of this material is also markedly influenced by the laser energy density. There are some discrepancies in the literature concerning the effect of the AM method on texture, shape memory properties and ageing effect induced by various processing methods, like LENS or EBAM [3-19]. Therefore in the present paper the effects of the AM methods on structure, shape memory properties and ageing are compared and discussed.

2. Experimental methods

The LENS method was used to prepare AM samples using the initial material in the form of spherical powder. During deposition, the powder was injected through the nozzles into the melt pool formed on the deposit surface by a highly focused laser beam. The deposition process was performed using the LENS MR-7 system (Optomec, USA) equipped with a 500 W fiber laser. Spherical, gas atomized powder, with particle size in the range of 45-115 μm and the chemical composition: 50.08 at.% Ni, 0.01 at.% C, 0.10 at.% O, Ti balance was used. In order to obtain cylindrical samples with 20 mm diameter and the height of 10 mm, the following parameters were used: laser power 400 W, laser spot diameter 1.2 mm, working table feed rate 10 mm/min, powder flow rate 14.98 g/min, single layer thickness 0.3 mm. Moreover, the process was performed in a chamber under a purified argon atmosphere (O_2 and H_2O < 10 ppm). Aging at 500°C was performed for times varied from 15 min to 8 h, as for typical heat treatment of Ni-rich Ni-Ti alloys [25], employed for the additive manufactured samples. The materials were analysed in the as-deposited and aged states.

The microstructural observations and Electron Backscatter Diffraction (EBSD) measurements were carried out on a FEI Versa 3D FEG scanning electron microscope (SEM) equipped with an EDAX Hikari CCD camera. The detailed microstructural studies were performed using a transmission electron microscope (TEM) Tecnai FEG G2 F20 Super Twin. The thin foils for TEM observations were prepared by electropolishing of 100 μm thick discs in an electrolyte containing 10 mol.% $HClO_4$ in methanol (voltage 20 V, temperature –20°C).

The tensile tests were performed at a Shimadzu Autograph AG-X plus testing machine at strain rate 10^{-3} s^{-1}. The strain was measured using a video-extensometer TRViewX system. Tests were conducted at RT and at temperature 10°C above austenite finish (A_f) of the materials. The samples for the tests were prepared in the same form as for in-situ deformation studies. The phase transformation temperatures were investigated by differential scanning calorimetry (DSC) using a Mettler DSC 823 instrument, with cooling/heating rate of 10°C/min.

3. Results and discussion

Fig. 1 shows a photograph of samples manufactured using various methods, i.e. LENS (a) and EBAM (b). It can be clearly seen that the LENS method allows for producing precise thin wall elements from a fine powder prepared by laser beam heating, while the EBAM method due to electron beam melting of 1 mm thickness wire shows effects of secondary melting and the walls of produced rectangular sample and are not as well shaped as those of the LENS sample.

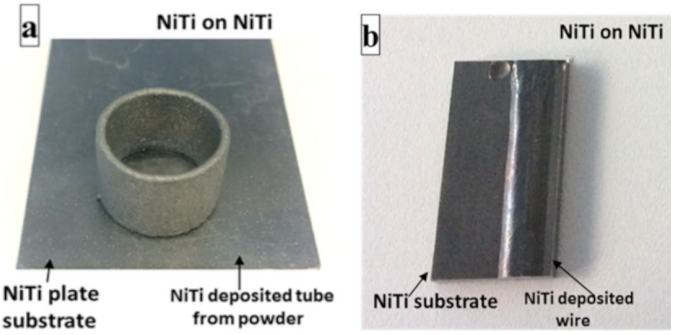

Fig. 1. (a) NiTi element deposited using LENS method; (b) NiTi element deposited from a wire on NiTi substrate using EBAM method

Fig. 2 shows DSC curves taken from LENS and EBAM prepared samples aged at 500°C. The as deposited samples show slightly different M_s temperatures, i.e. 4°C and –10°C respectively. After ageing these temperatures are shifted to a higher temperature range i.e. 16°C and 51°C. Correspondingly ageing at 500°C A_f temperatures are shifted after from 32°C (as deposited) to 48°C (8 h/500°C) for the LENS method and for the EBAM method from 20°C to 51°C. It was found that particularly for the medium time of ageing, the LENS samples show higher differences between appearance of the *R* phase that the EBAM samples. For both AM processing routes the ageing results in closer positions of martensite and *R* phase peaks. The ageing effects observed in the present work are in agreement with the previous works on aged NiTi alloys [20,21] and in our earlier studies of AM NiTi alloys [18,19].

Fig. 3 shows optical micrographs comparing microstructures of cross sections of (a) EBAM deposited sample from a NiTi wire and LENS deposited from the NiTi powder. Fig. 3a shows columnar grains of width similar to the width of the substrate and several hundred mm long. This may indicate oriented growth as observed earlier in Ref. [12,15,18,19,22] in the EBAM deposited layers. The microstructure of LENS deposited sample exhibits slightly different character; there exist a transition layer of fine grains that were likely remelted and subsequently fast cooled. The deposited layer shows elongated grains, however,

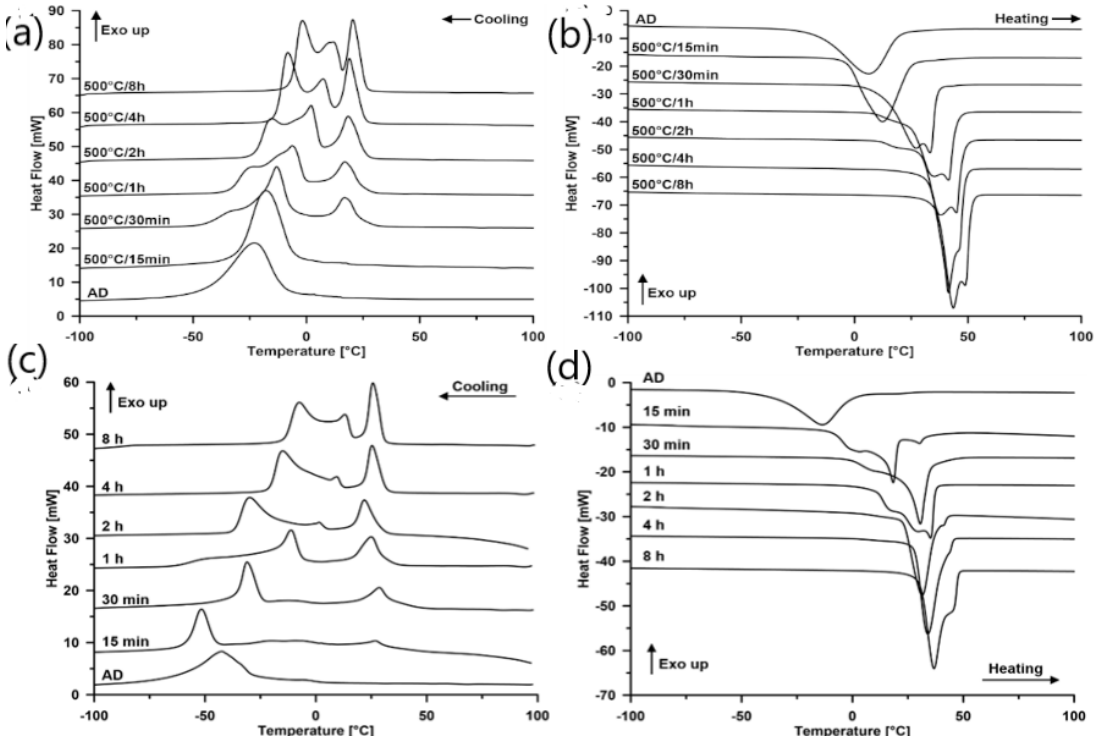

Fig. 2. DSC cooling (a) and heating (b) curves of the EBAM deposited NiTi and after various time of aging at 500°C and of the LENS deposited sample (c) cooling and (d) heating also with indicated ageing time

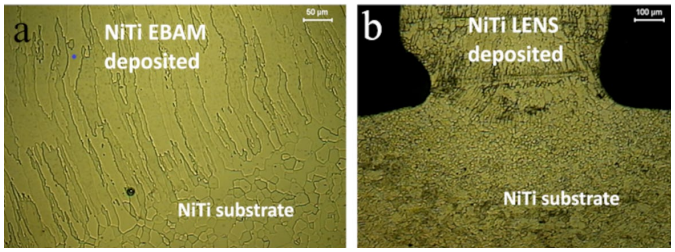

Fig. 3. (a) Optical microstructure of the cross section of deposited ring of EBAM deposited sample; (b) cross section of LENS deposited sample

shorter than in the case of EBAM method. It is in agreement with results of Hamilton et al. [6] where deposited layer showed random B2 austenitic grain orientations for the as built and solution treated alloys. The laser- based directed energy deposition LDED AM fabrication technique produces a characteristic grain morphology without texture. In other cases, weak texture was observed.

Fig. 4a shows the compressive stress-strain loading/unloading curves for the samples deposited using LENS technique and aged at 500°C/2 h. All samples underwent only partial strain recovery. The material in the as-deposited state revealed a good strain recovery (about 3%), which is in agreement with DSC results showing the A_f temperature below the deformation temperature (RT). The recoverable strain decreased to about 1.5% in the case of aged material, as a result of shift of the A_f toward higher temperature. Therefore, in order to determine the superelastic behavior above the A_f temperature, the compres-

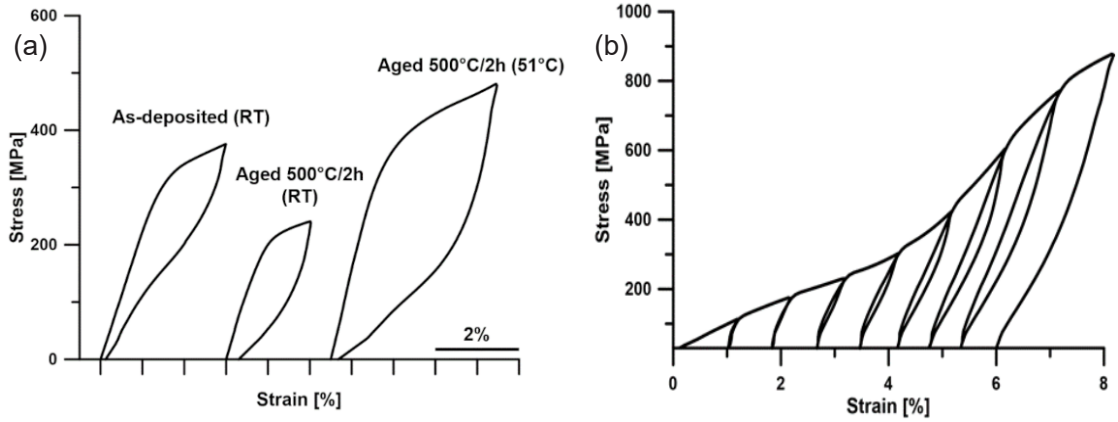

Fig. 4. Compression stress-strain curves (a) from directly LENS deposited NiTi samples aged at 500°C/2 h, tested at RT and 50°C as marked in brackets; (b) from NiTi EBAM deposited sample with increasing loading and unloading

sion test was performed at 51°C (10°C above A_f). The result shows almost complete strain recovery near 4% indicating almost perfect superelastic effect as observed also in AM shape memory materials [6,9], however, after heat treatment. Fig. 4b shows deformation/elongation curves taken from NiTi EBAM prepared samples with the increasing load in 8 steps from 100 to 900 MPa; each step followed by unloading showing typical curve for deformation of martensite typical for shape memory effect and no superelastic effect at room temperature was observed as described in Ref. [20].

In order to compare the preferred orientation after both processing methods, i.e. LENS and EBAM, EBSD orientation mapping was performed from the interfaces of deposited samples and 001 and 111 pole figures are shown in Figs. 5 and 6. In order to compare texture formation in both cases SEM electron back scattered diffraction studies EBSD were performed for both differently processed specimens on the surface perpendicular to the growth direction as indicated by an arrow in Fig. 6. It shows the inverse pole figure IPF map of the austenite grains in the as-deposited sample from a surface of a tensile sample with a marked square fragment where observation was performed with increasing strain. The image shows elongated grains, with majority in purple and orange colours indicating orientation not far from the [001] growth direction, as results from the austenite unit triangle where the [001] pole is in red color. The build direction is close to [001], the direction found in previous studies on AM manufactured NiTi alloys [13,14,16] where a cube texture was observed while an elongated grain curvature resulted from a nozzle movement during deposition. Pole figures were rotated to represent the deposition surface. One can see from IPF images that both samples show rather large grains in the deposited areas (in upper part of Fig. 5), however, looking more closely fine elongated subgrains of slightly different colors may be distinguished within these grains. The grains and subgrains in the EBAM deposited sample are considerably larger what resulted from different cooling conditions in larger melted areas. The grains of the EBAM sample exhibit colors closer to red since this color represents the 001 pole, while in the case of LENS sample various colors prevail in the substrate, but also in the deposited part i.e. blue (111 pole) and green (110 pole). These observations are in agreement with pole figures shown for both processing routes. The LENS prepared sample shows the spread of peaks, representing texture deviated by several degrees from (001)[100] orientation. Slightly different texture shows EBAM deposited sample where (001)[100] orientation is rotated a few degrees around [010] direction. The IPF map of the LENS prepared sample is similar to that reported in Ref. [12] where also [001] growth direction was reported and the deviation was explained by laser scan direction. Wang [14] reported that [001] texture is weakened by enhancing deposition current for dual-wire arc additive manufactured Ni-rich NiTi alloy. In the case of EBAM prepared sample the movement of electron beam seems to induce similar structural effects. As reported by Saedi [17], SLM fabricated samples showing the sharp [001] texture (the building direction) improve their superelastic response substantially. This is in agreement with our results for the LENS deposited sample where a good superelastic properties were well documented.

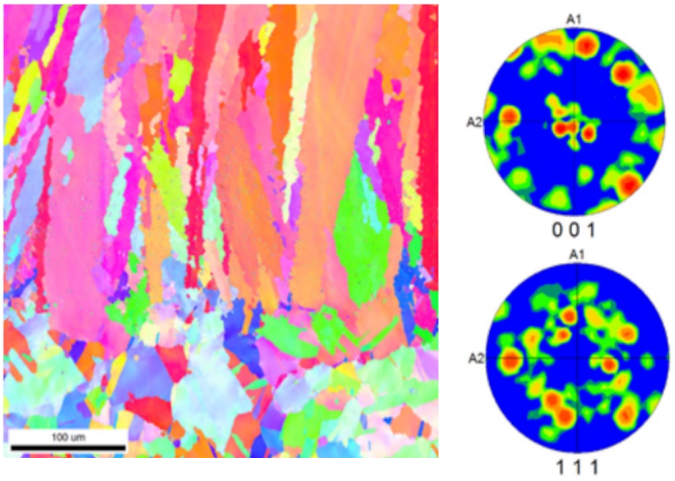

Fig. 5. EBSD orientation mapping above the interface from the LENS deposited sample and 001 and 111 pole figures rotated to represent the deposition surface

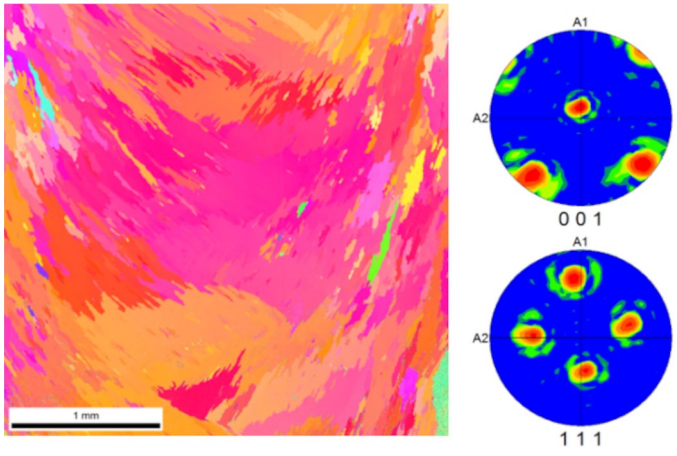

Fig. 6. EBSD orientation mapping above the interface from the LENS deposited sample and 001 and 111 pole figures rotated to represent the deposition surface

Fig. 7 shows TEM microstructure of the LENS deposited sample, where dark irregular particles of size between 500 nm - 2 μm are clearly visible. The electron diffraction pattern allows for identification of Ti_2Ni particles formed during cooling of the melt during preparation of the element. It is confirmed by the EDS analysis, where almost exactly it indicates atomic fraction of the Ti_2Ni compound. Such particles were previously reported as crystallizing from the liquid NiTi alloy [19,23].

Fig. 8 shows a STEM micrograph presenting elongated bright precipitates and a large dark particle. The EDS analysis from a dark particle (point 1) point to a Ti_2Ni primary particle as observed in Fig. 7, however elongated bright precipitates are most likely the Ni-rich precipitates visible also in the electron microstructure in Fig. 8. The electron diffraction pattern from the central part of the microstructure shows, however, only diffraction spots from the ordered austenite and twinned B19' martensite with 011 twinning plate as often observed in NiTi alloys [19,24].

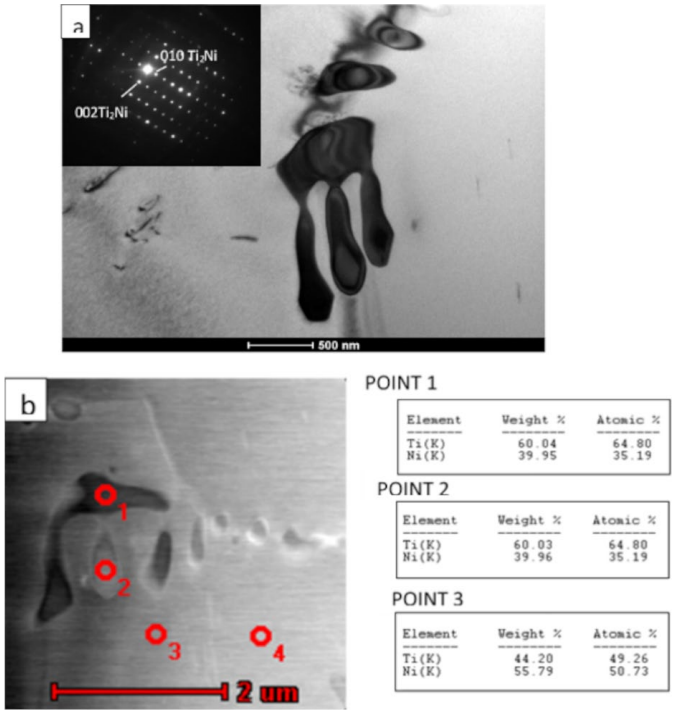

Fig. 7. (a) TEM microstructure of LENS deposited sample showing primary intermetallic particles; (b) STEM micrograph showing intermetallic particles and results of EDS analysis

The Ni-rich precipitates are coherent with the matrix showing strong strain field contrast and do not show other diffraction spots than those from the matrix. Fig. 9 shows TEM microstructure of EBAM manufactured sample. The microstructure is characterized by much higher density of martensitic plates due to a lower M_s temperature than that for the LENS deposited sample. The frequently observed martensitic twins show the similar orientation relationship with the matrix like that observed in Fig. 8 and

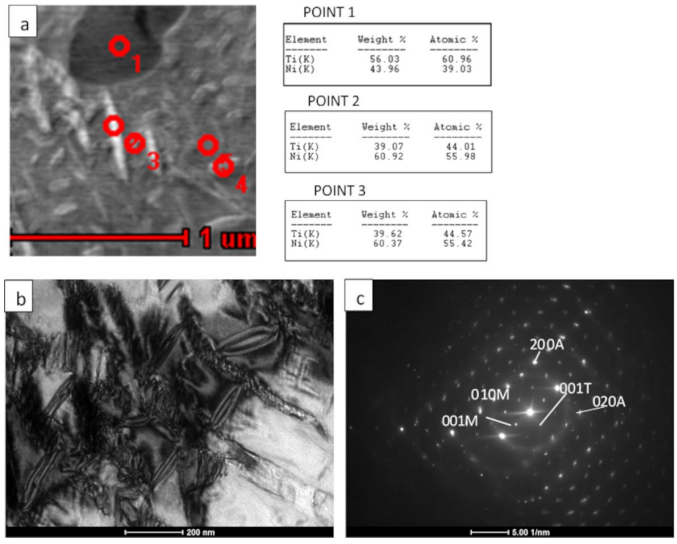

Fig. 8. TEM of LENS deposited sample aged 2h/500°C. (a) STEM micrograph showing two kinds of precipitates and tables showing results of a quantitative EDS analysis from points 1-3; (b) TEM microstructure and (c) Electron diffraction pattern from the central part of the microstructure

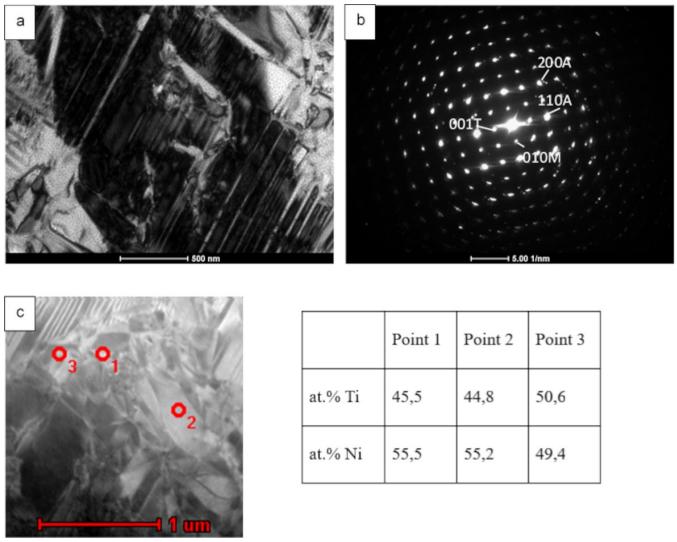

	Point 1	Point 2	Point 3
at.% Ti	45,5	44,8	50,6
at.% Ni	55,5	55,2	49,4

Fig. 9. (a) TEM microstructure from deposited rectangular element from NiTi alloy by EBAM method and (b) SADP from the central martensitic needles of [001] B2 zone axis orientation; (c) STEM micrograph showing primary particles martensite with marked 1-3 points and results of EDS analysis in the Table on the right side

the same twinning plane {011}. Small particles of the primary Ni-rich phase, are also visible in the microstructure. They are evidently different than the particles in the LENS sample, most likely due to different cooling conditions from the melt, resulting in a different crystal structure.

4. Summary

1. Samples prepared using the LENS method showed texture that is several degrees deviated from the <001> build direction, however, with composition close to the initial powder composition showing a superelastic effect. The EBAM manufactured sample showed martensitic structure at room temperature due to the larger shift of transformation temperatures to the higher range associated with a lower Ni content, resulted from processing conditions. However, EBAM method revealed the sharper <001> texture in the built direction and allowed for obtaining a good superelastic effect above the room temperature.
2. Intermetallic particles of size 0,5-2 μm, identified as Ti_2Ni using EDS and electron diffraction analysis, were observed often at grain boundaries. On the other hand the EBAM prepared sample showed Ni-rich particles due to different processing conditions causing loss of Ni in the solid solution and increase the martensitic transformation temperatures.

Ageing at 500°C shift the martensitic transformation temperatures to higher range in both, LENS and EBAM prepared samples. It resulted from the formation of Ni-rich coherent precipitates identified by STEM technique. In the as-prepared and aged samples the presence of martensite B19' twins was observed mainly on {011} B19' planes.

Acknowledgments

The presented research results are the effect of the project no. UMO-2016/23/B/ST8/00754 financed by the National Science Center, Poland.

REFERENCES

[1] M. Elahinia, N.S. Moghaddam, M.T. Andani, A. Amerinatanzi, B.A. Bimber, R.F. Hamilton, A Review, Prog. Mater. Sci. **83**, 630-663 (2016).

[2] D. Ding, Z. Pan, D. Cuiuri, H. Li, Int. J. Adv. Manuf. Tech. **81** (1-4), 465-481 (2015).

[3] T. Bormann, B. Műller, M. Schinhammer, A. Kessler, P. Thalmann, M. de Wild, Mater. Charact. **94**, 189-202 (2014).

[4] C. Wang, X.P. Tan, Z. Du, S. Chandra, Z. Sun, C.W.J. Lim, S.B. Tor, C.S. Lim, C.H. Wong, J. Mater. Process. Technol. **271**, 152-161 (2019).

[5] I.V. Shishkovsky, I.A. Yadroitsev, I.Y. Smurov, Technical Physics Letters **39**, 1081-1084 (2013).

[6] R.F. Hamilton, B.A. Bimber, T.A. Palmer, J. Alloys Compounds **739**, 712-722 (2018).

[7] I. Gibson, D. Rosen, B. Stucker, New York, 2015.

[8] J.P. Oliveira, A.J. Cavaleiro, N. Schell, A. Stark, R.M. Miranda, J.L. Ocana, F.M. Braz Fernandes, Scripta Materialia **152**, 122-126 (2018).

[9] S. Saedi, A.S. Turabi, M.T. Andani, C. Haberland, H. Karaca, M. Elahinia, J. Alloyd Compounds **677**, 204-210 (2016).

[10] C. Ma, D. Gu, D. Dai, M. Xia, H. Chen, Materials Characterization **143**, 191-196 (2018).

[11] J.J. Marattukalam, V.K. Balla, M. Das, S. Bontha, S.K. Kalpathy, J. Alloy Compounds **744**, 337-346 (2019).

[12] S. Kumar, L. Marandi, V.K. Balla, S. Bysakh, D. Piorunek, G. Eggeler, M. Das, I. Sen, Materialia **8**, 100456 (2019).

[13] Z. Zeng, J.P. Oliveira, S. Ao, W. Zhang, J. Cui, S. Yan, B. Peng, Optics & Laser Technol. **122**, 105876 (2020).

[14] J. Wang, Z. Pan, Y. Wang, L. Wang, S. Su, D. Cuiuri, Y. Zhao, H. Li, Additive Manufacturing **34**, 101240 (2020).

[15] J. Dutkiewicz, Ł. Rogal, D. Kalita, M. Węglowski, S. Błacha, K. Berent, T. Czeppe, A. Antolak-Dudka, T. Durejko, T. Czujko, J. Mater. Eng. Perf. **29**, 4463-4473 (2020).

[16] M. Elahinia, N.S. Moghaddam, M.T. Andani, A. Amerinatanzi, B.A. Bimber, R.F. Hamilton **83**, 630-663 (2016).

[17] S. Saedi, A.S. Turabi, M.T. Andani, N.S. Moghaddam, M. Elahinia, H.E. Karaca, Mater. Sci. Eng. A, **686**, 1-10.

[18] J. Dutkiewicz, Ł. Rogal, D. Kalita, J. Kawałko, M. Węglowski, K. Kwieciński, P. Śliwiński, H. Danielewski, B. Antoszewski, E. Cesari, J. Mater. Eng. Perf. **31**, 1609-1621 (2022).

[19] J. Dutkiewicz, Ł. Rogal, D. Kalita, K. Berent, J. Kawałko, A. Antolak-Dudka, T. Durejko, T. Czujko, E. Cesari, J. Mater. Science Metallurgy **2**, 1-7 (2021) open access.

[20] H. Morawiec, Wydawnictwo Uniwersytetu Śląskiego, Katowice, 2014.

[21] I. Kaya, H.E. Karaca, M. Nagasako, R. Kainuma, Mater. Character. **159** 110034 (2020).

[22] Q. Zhou, M.D. Hayat, G. Chen, S. Cai, X. Qu, H. Tang, P. Cao, Mater. Sci. Eng. A. **744**, 290-298 (2019).

[23] J. Bhagyaraj, K.V. Ramaiah, C.N. Saikrishna, S.K. Bhaumik, Gouthama, J. Alloy Compounds **581**, 344-351 (2013).

[24] Bin Li, Yidi Shen, Qi An, Acta Met. **199**, 240-252 (2020).